TOWARDS FAST ORBIT CORRECTION: A MODULAR AND EXTENSIBLE GLOBAL ORBIT FEEDBACK SYSTEM

A. Aljadaa*, A. Ahmad, A. Abbadi, H. Al-Mohammad, M. Attal, S. Kasaei
SESAME Synchrotron, Allan, Jordan

Abstract

At SESAME, orbit correction was previously performed every 5 seconds (0.2 Hz) using MATLAB. However, due to the limited correction speed and MATLAB's unsuitability for production environments, a complete in-house implementation of the system was undertaken using the C programming language. This migration enabled significantly faster correction, a modular architecture to support various control and estimation algorithms, and feedforward control.

INTRODUCTION

At SESAME, the orbit feedback system was redesigned to address the limitations of the previous MATLAB-based implementation, which operated at only 0.2 Hz. The new system, implemented in C, achieves sampling rates up to 10 Hz, enabling correction of higher-frequency disturbances that were previously unaddressable.

The system architecture was designed with modularity as a core principle, facilitating easy modification and integration of different control and estimation algorithms. The complete ecosystem comprises multiple integrated components: C-based core implementation for orbit correction, an EPICS Input/Output Controller (IOC) for process variable management, a Qt-based graphical user interface for system monitoring and control, Python scripts for offline performance evaluation, and MATLAB/Simulink tools for system simulation and controller tuning.

SYSTEM LAYOUT

The orbit feedback system consists of three primary software components that work in concert to achieve orbit correction: a C-based core correction engine, an EPICS IOC, and a Qt-based graphical user interface.

The core correction engine, implemented in C, executes the orbit feedback algorithm at a 10 Hz sampling rate. This component reads slow acquisition (SA) beam position data from the Beam Position Monitors (BPMs) electronics (Libera Brilliance + [1]), applies the selected estimation and control algorithms, and computes the corresponding corrector magnet current setpoints. The modular design allows configurable selection of different controllers and state estimators.

The EPICS IOC [2] serves as the interface layer between the correction engine and the control system infrastructure. It exposes all relevant process variables for both monitoring and configuration, including BPM readings, corrector setpoints, controller gains, and diagnostic signals.

* amro.aljadaa@sesame.org.jo

The Qt-based graphical user interface provides operators with comprehensive system visualization and control capabilities. The GUI displays live orbit data in multiple representations: time-domain waveforms for tracking transient behavior, frequency-domain spectra for identifying harmonic disturbances, and spatial orbit distributions for visualizing beam position at all BPM locations. For postmortem analysis, time-resolved plots enable detailed investigation of system behavior following fault conditions. Configuration parameters can also be adjusted through the GUI.

CONTROL SYSTEM DESIGN

The orbit feedback system employs a Singular Value Decomposition (SVD) based correction algorithm [3] to compute optimal corrector magnet current setpoints. This approach decomposes the orbit response matrix into orthogonal eigenmodes, enabling decoupled correction of individual orbit modes while providing inherent numerical stability.

The fundamental correction equation relates the required corrector current changes to the measured orbit deviations:

$$\Delta I = V \cdot S_{\text{inv}} \cdot C_z \cdot U^T \cdot \Delta x,$$

where ΔI is the vector of corrector current changes, Δx represents the orbit error relative to the golden orbit, U and V are the left and right singular vectors of the orbit response matrix, S_{inv} is a diagonal matrix containing the inverse singular values with regularization, and C_z is the controller transfer function in discrete time (z-domain). The SVD formulation allows selective mode correction and natural implementation of Tikhonov regularization [4].

The system incorporates RF frequency adjustment as a primary correction mechanism. Changes in RF frequency modulate beam energy to match the design energy. RF correction is applied first to stabilize beam energy, followed by corrector magnets for fine orbit adjustment. This approach reduces the correction load on the magnets and prevents corrector saturation.

Figure 1 illustrates the control loop architecture. The control system integrates several components: state estimation to filter noisy BPM measurements, feedback control for steady-state and dynamic correction, and feedforward compensation for predictable disturbances. Additionally, regularization techniques are implemented to prevent excessive corrector activity.

Estimator

Raw BPM measurements can contain noise from various sources. To address this, the system implements three selectable state estimation algorithms, each offering different tradeoffs between noise rejection and response time.

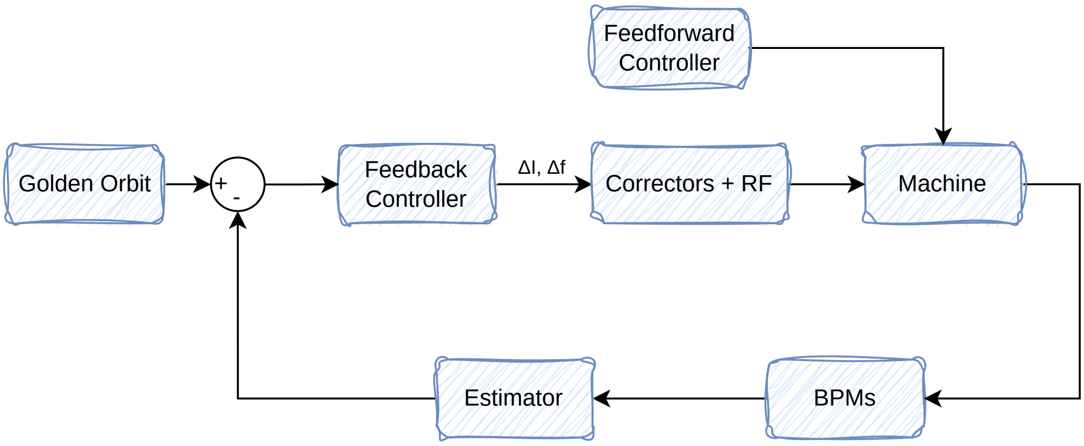

Figure 1: Orbit correction system architecture.

The Moving Average (MA) filter computes a simple arithmetic mean over a sliding window of N samples:

$$\hat{x}[k] = \frac{1}{N}\sum_{i=0}^{N-1} x[k-i].$$

This approach provides straightforward noise reduction but introduces latency approximately half the window length.

The Exponentially Weighted Moving Average (EWMA) filter applies exponentially decaying weights to past measurements:

$$\hat{x}[k] = \alpha \cdot x[k] + (1-\alpha) \cdot \hat{x}[k-1],$$

where $\alpha \in (0,1)$ controls the weighting between new measurements and previous estimates, with larger values providing faster response and smaller values providing heavier filtering. This recursive structure requires minimal memory and computational effort while providing tunable filtering characteristics through adjustment of the weighting parameter.

For applications requiring optimal noise rejection, a discrete Kalman filter can be used, which provides theoretically optimal estimates when noise statistics are properly characterized.

The modular software architecture enables configurable selection between estimation algorithms or complete bypass of the estimation stage. Filter parameters including window size and smoothing factor are adjustable through the graphical user interface. This plug-and-play capability facilitates rapid algorithm comparison and system tuning during commissioning and operation. The estimation module can be enabled for specialized studies, commissioning activities, or investigations where additional signal processing may be beneficial.

Feedback Controller

The feedback controller implements a Proportional-Integral (PI) control law in discrete time. The PI controller provides both immediate response to orbit errors through the proportional term and elimination of steady-state errors through the integral term. The discrete-time PI controller in the z-domain is represented as:

$$C_z = K_p + K_i T_s \frac{z}{z-1},$$

where K_p is the proportional gain, K_i is the integral gain, and T_s is the sampling period.

The derivative (D) term commonly found in PID controllers is intentionally excluded. Derivative action amplifies high-frequency noise and can lead to excessive corrector activity when applied to noisy BPM measurements. Since the system already achieves adequate disturbance rejection and stability margins with PI control, the added complexity and noise sensitivity of derivative action is unnecessary.

The gain structure implements a two-level hierarchy to provide both global and local control authority. Global proportional and integral gains are configured through the graphical user interface, providing convenient adjustment of the overall loop response. Additionally, the system provides the capability to fine-tune each individual gain independently, enabling localized correction adjustments for specific orbit locations that may be particularly sensitive or prone to disturbances.

This flexible gain structure allows us to maintain aggressive correction at critical locations while applying gentler control elsewhere, optimizing both orbit stability and corrector efficiency across the storage ring.

Feedforward Controller

In addition to feedback correction, the system implements feedforward compensation to preemptively counteract known disturbance sources. The primary application targets orbit disturbances induced by insertion devices.

Insertion devices such as wigglers and undulators produce strong magnetic fields that vary with gap and shift changes. As users adjust these parameters during experiments, the resulting field changes introduce predictable orbit distortions.

Rather than relying solely on feedback to correct these disturbances after they occur, feedforward table compensation applies precalculated corrector adjustments simultaneously with the parameter changes, significantly reducing transient orbit excursions.

The feedforward implementation employs Python scripts that monitor insertion device positions via EPICS process variables and compute appropriate corrector setpoints using pre-measured lookup tables. Interpolation provides smooth corrector trajectories as gaps and shifts move continuously.

Regularization

The SVD-based correction algorithm requires inversion of the singular value matrix, which can lead to excessive corrector currents when small singular values are present. Small singular values correspond to orbit modes that are weakly controllable or observable, and their inversion amplifies measurement noise into large corrector demands that may exceed physical limits or cause instability.

Two approaches are implemented to address this ill-conditioned inverse problem. The first employs SVD truncation, where singular values below a specified threshold are entirely excluded from the correction, effectively discarding weakly controllable modes. The second applies Tikhonov regularization, which adds a damping parameter to the singular value inversion:

$$S_{inv,ii} = \frac{S_{ii}}{S_{ii}^2 + \lambda^2},$$

where S_{ii} are the singular values and λ is the regularization parameter selected through empirical tuning during commissioning. This modification smoothly attenuates the contribution of small singular values, preventing large corrector demands.

The modular implementation allows adjustment of the regularization parameter through the GUI or complete disabling of regularization, enabling us to adapt the correction strategy to changing operational conditions without recompiling the core correction engine.

FUTURE WORK

The current implementation operating at 10 Hz sampling rate represents an intermediate step toward achieving true Fast Orbit Feedback (FOFB) capabilities. Several enhancements are planned to advance the system toward higher sampling rates.

Notch filtering will be integrated into the feedforward controller to suppress power line harmonics at 50 Hz and associated multiples, further reducing residual orbit disturbances from electromagnetic interference.

A MATLAB Simulink simulation environment is currently under development to enable offline testing and validation of control algorithms before deployment to the operational system. This will facilitate rapid prototyping and parameter optimization for future FOFB implementations.

Preparatory work towards FOFB has already been completed, including fast BPM data acquisition software. The modular architecture supports integration of FPGA solutions for hardware-accelerated computation at higher rates.

The ultimate goal is transition to FOFB operation [5] at significantly higher sampling rates, enabling correction of faster disturbances and improved orbit stability. This upgrade requires completion of fast data acquisition infrastructure across all BPM locations in the storage ring. The modular software architecture will facilitate rapid integration of FOFB algorithms without requiring fundamental redesign of the control system framework.

CONCLUSION

An improved orbit feedback control system has been successfully designed, implemented, and deployed at SESAME to address the limitations of the previous MATLAB-based implementation. The migration to C-based implementation enabled a 50-fold increase in sampling rate, from 0.2 Hz to 10 Hz, significantly improving the system's ability to correct higher-frequency orbit disturbances.

The modular software architecture provides plug-and-play capability for different estimation algorithms, control strategies, and regularization techniques. This design philosophy enables rapid algorithm evaluation and system tuning without requiring code recompilation, substantially reducing development and commissioning time.

The complete ecosystem integrates C-based correction, EPICS infrastructure for control system integration, Qt-based graphical interfaces for operator monitoring, and Python-based tools for performance evaluation. This comprehensive approach addresses all aspects of orbit feedback system operation from implementation through commissioning to long-term performance assessment.

The system has been successfully deployed in production, demonstrating improved orbit quality. As indicated by the title, this implementation establishes the foundation for future Fast Orbit Feedback capabilities, with the modular framework designed to accommodate higher sampling rates.

REFERENCES

[1] H. Al-Mohammad and K. Manukyan, "SESAME storage ring diagnostics and commissioning", in *Proc. IBIC'17*, Grand Rapids, MI, USA, Aug. 2017, pp. 16–20. doi:10.18429/JACoW-IBIC2017-MO2AB3

[2] "EPICS: Experimental Physics and Industrial Control System". https://epics-controls.org

[3] M. Muñoz, Z. Martí, D. Einfeld, and G. Benedetti, "Orbit studies during ALBA commissioning", in *Proc. IPAC'11*, San Sebastián, Spain, Sep. 2011, paper THPC056, pp. 3020–3022.

[4] M. T. Heron *et al.*, "Diamond light source electron beam position feedback", in *Proc. ICALEPCS'09*, Kobe, Japan, Oct. 2009, paper THB003, pp. 650–652.

[5] J. Chen *et al.*, "Status of SSRF fast orbit feedback system", in *Proc. IPAC'13*, Shanghai, China, May 2013, paper WEPME033, pp. 2995–2997.